

STABILITY ANALYSIS FOR 3D FRAMES USING MIXED COROTATIONAL FORMULATION

Rabe Alsafadie*, Mohammed Hjiat* and Jean-Marc Battini**

* Structural Engineering Research Group/LGCGM, INSA de Rennes, 20 avenue des Buttes de Coësmes
35043 Rennes Cedex France

e-mails: Rabe.Alsafadie@insa-rennes.fr, Mohammed.Hjiat@insa-rennes.fr

** Department of Civil and Architectural Engineering, KTH, Royal Institute of Technology, SE-10044
Stockholm, Sweden

e-mail: Jean-Marc.Battini@sth.kth.se

Keywords: Geometrically nonlinear, 3D beams, corotational formulation, mixed finite element analysis, arbitrary cross-sections, elasto-plastic material behavior, Hellinger-Reissner functional.

***Abstract.** The corotational technique is adopted for the analysis of 3D beams. The technique applies to a two-noded element a coordinate system which continuously translates and rotates with the element. In this way, the rigid body motion is separated out from the deformational motion. Then, a mixed formulation is adopted for the derivation of the local element tangent stiffness matrix and nodal forces. The mixed finite element formulation is based on an incremental form of the two-field Hellinger-Reissner variational principle to permit elasto-plastic material behavior. The proposed element can be used to analyze the nonlinear buckling and postbuckling of 3D beams. The mixed formulation solution is compared against the results obtained from a corotational displacement-based formulation having the same beam kinematics. The superiority of the mixed formulation is clearly demonstrated.*

1 INTRODUCTION

In recent literature, there have been notable contributions to improve the accuracy and efficiency of displacement-based finite elements. This approach has the limitation in elasto-plasticity since the approximations of the axial strains and curvatures are constrained by the element's assumed displacement fields. Nonetheless, these curvatures can vary in a highly nonlinear fashion along the length of an elasto-plastic structural member. For example, Izzuddin and Smith [1] found that a large number of displacement-based beam finite elements are typically required to represent elasto-plasticity behavior accurately. In the mixed formulation, both internal forces and displacements are interpolated independently. This formulation addresses the fundamental limitation of conventional displacement-based elements: the inability of simple displacement polynomials to represent the highly nonlinear distribution of the curvatures along the member lengths due to general distributed yielding.

The corotational approach has been recently adopted by several authors to handle the geometric nonlinearity in 3D displacement-based beam models (Alsafadie et al. [2], [3], Battini and Pacoste [4], [5], Crisfield and Moita [6]). This paper extends the works of Battini on corotational beam elements by applying the two-field Hellinger-Reissner variational principle for the development of a mixed local formulation. The corotational approach is employed to handle the geometric nonlinearity, where, in the corotational frame, the element rigid body motion has been removed and the formulations focus solely on the element deformational degrees of freedom.

2 COROTATIONAL FRAMEWORK FOR 3D BEAMS

The central idea in the corotational formulation for a two-noded 3D beam is to introduce a local coordinate system which continuously rotates and translates with the element. Then, local deformational displacements \mathbf{d}_l are defined by extracting the rigid body movements from the global displacements \mathbf{d}_g . The local displacements are expressed as functions of the global ones, i.e.

$$\mathbf{d}_l = \mathbf{d}_l(\mathbf{d}_g) \quad (1)$$

Then, \mathbf{d}_l is used to compute the internal force vector \mathbf{f}_l and tangent stiffness matrix \mathbf{K}_l in the local frame. The transformation matrix \mathbf{B} between the local and global displacements is defined by

$$\delta \mathbf{d}_l = \mathbf{B} \delta \mathbf{d}_g \quad (2)$$

and is obtained by differentiation of (1). The expression of the internal force vector in global coordinates \mathbf{f}_g and the tangent stiffness matrix \mathbf{K}_g in global coordinates can be obtained by equating the internal virtual work in both the global and local systems, i.e.

$$\mathbf{f}_g = \mathbf{B}^T \mathbf{f}_l, \quad \mathbf{K}_g = \mathbf{B}^T \mathbf{K}_l \mathbf{B} + \partial(\mathbf{B}^T \mathbf{f}_l) / \partial \mathbf{d}_g \Big|_l \quad (3)$$

Relations (1), (2) and transformations (3) are explained in details in [4].

3 NONLINEAR BERNOULLI MIXED LOCAL ELEMENT FORMULATION

In this section, the internal force vector \mathbf{f}_l and tangent stiffness matrix \mathbf{K}_l of a mixed local element formulation based on the kinematics assumption of the Bernoulli beam theory are derived.

3.1 Kinematics and local displacements interpolations

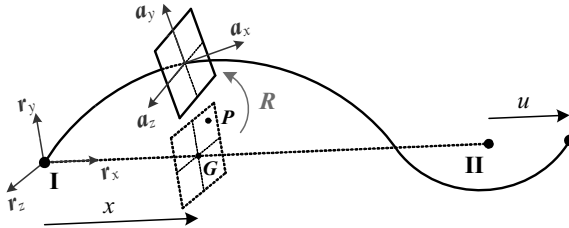


Figure 1: Local beam configuration.

Let $\mathbf{x}_p^0(x, y, z)$ denote the position vector of an arbitrary point P in the initial configuration and let $\mathbf{x}_p(x, y, z)$ denote the position vector of P in the current configuration (see figure 1).

$$\begin{aligned} \mathbf{x}_p^0(x, y, z) &= \mathbf{x}_G^0(x) + y \mathbf{r}_y + z \mathbf{r}_z \\ \mathbf{x}_p(x, y, z) &= \mathbf{x}_G(x) + y \mathbf{a}_y(x) + z \mathbf{a}_z(x) + \alpha(x) \bar{\omega}(y, z) \mathbf{a}_x(x) \end{aligned} \quad (4)$$

where \mathbf{x}_G^0 and \mathbf{x}_G denotes the position vectors of the centroid G in the initial and current configurations, respectively. In the case of thin-walled open cross-sections, the normalized warping displacement is expressed as the product of the warping parameter $\alpha(x)$ and the warping function $\bar{\omega}(y, z)$. To handle in a convenient way nonsymmetric cross-sections with distinct shear center and centroid, the warping function $\bar{\omega}$ is defined according to Saint-Venant torsion theory and refers to the centroid G , [7]:

$$\bar{\omega}(y, z) = \omega - y_c z + z_c y \quad (5)$$

and ω refers to the shear center defined by its coordinates y_c, z_c . The orthonormal triad $\mathbf{a}_i, i = (x, y, z)$ which specifies the orientation of the current cross-section, is given by

$$\mathbf{a}_i = \mathbf{R} \mathbf{r}_i, i = (x, y, z) \quad (6)$$

The rotation defined by the matrix \mathbf{R} can be considered as the sum of two bending rotations and a twist rotation, and given by (cf. [8]).

$$\mathbf{R} = \begin{bmatrix} 1 & -v_{,x} - w_{,x} \vartheta_x & -w_{,x} + v_{,x} \vartheta_x \\ v_{,x} & 1 & -\vartheta_x \\ w_{,x} & \vartheta_x & 1 \end{bmatrix} \quad (7)$$

where v, w and ϑ_x are the transverse displacements and the twist rotation of the cross-section centroid relative to the local coordinates system, respectively. Introducing the local rotation matrix defined in (7) into(4), the displacement vector can be evaluated as

$$\begin{aligned} U &= u - y(v_{,x} + w_{,x} \vartheta_x) - z(w_{,x} - v_{,x} \vartheta_x) + \bar{\omega} \alpha \\ V &= v - z \vartheta_x \\ W &= w + y \vartheta_x \end{aligned} \quad (8)$$

To obtain the strain vector the following assumptions are adopted: the nonlinear shear strain components generated by warping are omitted since warping effects are rationally taken into account in a linearized way only, the warping deformations are proportional to the variation of the torsional angle (Vlasov assumption), an average value of the axial strain is taken in order to avoid membrane locking and finally the nonlinear terms in the expressions of the bending curvatures and are neglected. With these modifications, the following strain expressions are obtained:

$$\begin{aligned} \varepsilon_{xx} &= \varepsilon_{av} - y \kappa_z + z \kappa_y + \frac{1}{2} (r^2 - \frac{I_o}{A}) \kappa_x^2 + \omega \kappa_{x,x} \\ 2\varepsilon_{xy} &= (\bar{\omega}_{,y} - z) \kappa_x \\ 2\varepsilon_{xz} &= (\bar{\omega}_{,y} - z) \kappa_x \end{aligned} \quad (9)$$

with $\kappa_x = \vartheta_{x,xx}, \kappa_y = -w_{,xx} - y_c \vartheta_{x,xx}, \kappa_z = v_{,xx} - z_c \vartheta_{x,xx}$

and $r^2 = (z^2 + y^2), \varepsilon_{av} = \frac{1}{L} \int_L \left[u_{,x} + \frac{1}{2} \left(v_{,x}^2 + w_{,x}^2 + \frac{I_o}{A} \vartheta_{x,x}^2 \right) \right] dx, I_o = \int_A r^2 dA$

Since the strain field in (9) is obtained from the local displacement field \mathbf{d}_l , therefore, all the components of the strain vector deduced from \mathbf{d}_l will be designated with a superimposed hat and combined as $\hat{\boldsymbol{\varepsilon}} = (\hat{\varepsilon}_{xx}, 2\hat{\varepsilon}_{xy}, 2\hat{\varepsilon}_{xz})$. Based on the above expression for strain vector idealization, the strain at any point in the cross-section of the beam element can be related to the cross-sectional generalized strain vector $\hat{\boldsymbol{\varepsilon}} = (\varepsilon_{av}, \kappa_y, -\kappa_z, \frac{1}{2} \kappa_x^2, \kappa_{x,x}, \kappa_x)$ as

$$\hat{\boldsymbol{\varepsilon}} = \mathbf{A}(y, z) \hat{\boldsymbol{\varepsilon}}(x) \quad (10)$$

In the present formulation, the axial rotation ϑ_x is interpolated with shape functions based on the closed-form solution of the torsional equilibrium equation for an elastic prismatic and geometrically linear beam. Cubic Hermitian shape functions are chosen for the transverse displacement v and w of the

centroid of the cross-section relative to the local element axes. And finally, linear interpolation is adopted for the axial elongation u of the local element. Thus, the variation in the cross-section deformation $\hat{\mathbf{e}}$ can be written as $\delta\hat{\mathbf{e}} = \mathbf{N}_e \delta\mathbf{d}_l$. Hence, an infinitesimal change in strain vector can be written as

$$\delta\hat{\mathbf{e}} = \mathbf{A}\mathbf{N}_e \delta\mathbf{d}_l \tag{11}$$

3.2 Equilibrium and generalized stress interpolation functions

The generalized stress resultants vector \mathbf{S} , which is work conjugate to the generalized strains $\hat{\mathbf{e}}$, may be expressed in vector form as $\mathbf{S}=(N\ M_y\ M_z\ B\ \Omega\ T_{sv})$ where N is conjugate to ϵ_{av} , M_y and M_z are conjugate to κ_y and κ_z , respectively. The bimoment B , Wagner stress resultant Ω , and the uniform torque T_{sv} are conjugate to $\kappa_{x,x}$, $\kappa_x^2/2$ and κ_x , respectively. Within each element, the generalized stress resultant internal force vector is approximated as

$$\mathbf{S} = \mathbf{N}_{s1} \mathbf{f}_s \tag{12}$$

where $\mathbf{f}_s = (N\ M_y^I\ M_z^I\ B^I\ T\ \Omega\ M_y^{II}\ M_z^{II}\ B^{II})$ the corotational force degrees of freedom of the mixed formulated element (where I: first node, II: second node and T a constant torque) and \mathbf{N}_{s1} is the force shape functions matrix satisfying the equilibrium equations.

$$\mathbf{N}_{s1} = \begin{bmatrix} 1 & 0 & 0 & 0 & 0 & 0 & 0 & 0 & 0 \\ w & 1-x/L & 0 & 0 & 0 & -x/L & 0 & 0 & 0 \\ v & 0 & x/L-1 & 0 & 0 & 0 & x/L & 0 & 0 \\ 0 & 0 & 0 & 0 & 0 & 0 & 0 & 0 & 1 \\ 0 & 0 & 0 & f_B^I & 0 & 0 & 0 & f_B^{II} & 0 \\ 0 & 0 & 0 & f_{B,x}^I & 1 & 0 & 0 & f_{B,x}^{II} & 0 \end{bmatrix} \tag{13}$$

where $f_B^I = -\frac{\sinh[k(L-x)]}{\sinh(kL)}$, $f_B^{II} = \frac{\sinh(kx)}{\sinh(kL)}$ and $k = \sqrt{\frac{GJ}{EI_\omega}}$

The resulting element will subsequently be termed as *bmw3d* element. It should be mentioned that relation (12) includes P - δ effects in the internal moment fields, based on the interpolated transverse displacements. The variation of the generalized stress resultant internal force vector, may be expressed as

$$\delta\mathbf{S} = \mathbf{N}_{s2} \delta\mathbf{d}_l + \mathbf{N}_{s1} \delta\mathbf{f}_s \tag{14}$$

3.3 Hellinger-Reissner potential for beams

In the Hellinger-Reissner mixed formulation, both the displacement and the internal forces are approximated by independent shape functions. This principle is applied to a beam element of length L loaded by end forces only. This two-field variational principle yields two sets of nonlinear equations

$$\mathbf{E}_Q = \int_L \mathbf{N}_e^T \mathbf{S} \, dx + \int_L \mathbf{N}_{s2}^T (\hat{\mathbf{e}} - \mathbf{e}) \, dx - \mathbf{F}_l^{ext} = 0 \tag{15}$$

$$\mathbf{E}_C = \int_L \mathbf{N}_{s1}^T (\hat{\mathbf{e}} - \mathbf{e}) \, dx = 0 \tag{16}$$

where \mathbf{E}_Q and \mathbf{E}_C are the element equilibrium and element strain-displacement compatibility equations, respectively. A third equation, the cross-section equilibrium, may be expressed as

$$\mathbf{S}_Q = \mathbf{S}_\Sigma - \mathbf{S} = 0 \tag{17}$$

where \mathbf{S}_Σ is given by the nonlinear cross-section constitutive relation and represents a general function that permits the computation of cross-section stress resultants for given cross-section deformations. The linearization of the cross-section constitutive relation $\mathbf{S}_\Sigma = \mathbf{S}_\Sigma(\mathbf{e})$ is obtained using the cross-section tangent stiffness matrix $\mathbf{k} = \partial\mathbf{S}_\Sigma / \partial\mathbf{e}$. The cross-section tangent exhibity matrix \mathbf{q} is obtained by inverting the cross-section tangent stiffness matrix: $\mathbf{q} = \mathbf{k}^{-1}$. Furthermore, \mathbf{S} is the interpolated generalized stresses acting over a cross-section and defined by (12).

3.4 Linearization of the Hellinger-Reissner functional

The nonlinear system of equations $\mathbf{E}_Q = \mathbf{0}$, $\mathbf{E}_C = \mathbf{0}$ and $\mathbf{S}_Q = \mathbf{0}$ may be solved using various combinations of Newton iteration at the element, and cross-section levels. Since interelement compatibility is not enforced for the generalized stress variables interpolation, the nonlinear discretized strain-displacement compatibility equation $\mathbf{E}_C = \mathbf{0}$ can be solved iteratively at the element level for every global equilibrium iteration. Similarly, the nonlinear constitutive equation $\mathbf{S}_Q = \mathbf{0}$ can be solved iteratively at the cross-section level for every element level iteration. In the following Subsections, the consistent linearization of the above nonlinear equations is presented. In the process of consistent linearization, it is important to recognize the arguments of any given function.

3.4.1 Linearization of the Cross-section Constitutive Equation

By expanding $\mathbf{S}_Q = \mathbf{0}$ about the current cross-section state while holding \mathbf{S} constant, we can write

$$\mathbf{S}_Q^{j+1} \approx \mathbf{S}_Q^j + \frac{\partial\mathbf{S}_Q}{\partial\mathbf{e}} \Delta\mathbf{e}^j \Rightarrow \Delta\mathbf{e}^j = -\mathbf{q}\mathbf{S}_Q^j = \mathbf{q}(\mathbf{S} - \mathbf{S}_\Sigma^j) \quad (18)$$

3.4.2 Linearization of the Element Compatibility Equation

The incremental form of the element compatibility condition $\mathbf{E}_C = \mathbf{0}$ may also be derived by taking a Taylor series expansion of $\mathbf{E}_C = \mathbf{0}$ about the current state variables \mathbf{f}_s and \mathbf{d}_l

$$\mathbf{E}_C^{i+1} \approx \mathbf{E}_C^i + \frac{\partial\mathbf{E}_C}{\partial\mathbf{d}_l} \Delta\mathbf{d}_l^i + \frac{\partial\mathbf{E}_C}{\partial\mathbf{f}_s} \Delta\mathbf{f}_s^i = \mathbf{0} \quad (19)$$

Then, solving for $\Delta\mathbf{f}_s^i$, we obtain

$$\Delta\mathbf{f}_s^i = \mathbf{H}_{11}^{-1} [(\mathbf{M}_\kappa + \mathbf{G}_1 - \mathbf{H}_{12})\Delta\mathbf{d}_l^i + \mathbf{E}_C^i] \quad (20)$$

3.4.3 Linearization of the Element Equilibrium Equation

Although the linearization of the discrete weak-form of the element equilibrium equation $\mathbf{E}_Q = \mathbf{0}$ follows standard procedure [35, 36], this linearization is complicated by the presence of displacement-dependent nonlinear interpolation functions for the generalized stresses. For the case at hand, the consistent local tangent stiffness equations are obtained by expanding (15) for each of the state variables \mathbf{d}_l , \mathbf{f}_s and $\mathbf{F}_l^{\text{ext}}$ about the current state. Again, a Taylor series expansion of $\mathbf{E}_Q = \mathbf{0}$ is written as follows

$$\mathbf{E}_Q^{n+1} \approx \mathbf{E}_Q^n + \frac{\partial\mathbf{E}_Q}{\partial\mathbf{d}_l} \Delta\mathbf{d}_l^n + \frac{\partial\mathbf{E}_Q}{\partial\mathbf{f}_s} \Delta\mathbf{f}_s^n - \Delta\mathbf{F}_l^{\text{ext},n} = \mathbf{0} \quad (21)$$

This equation can be rewritten by substituting $\Delta\mathbf{f}_s^n$ from (20), and solving for $\Delta\mathbf{d}_l^n$. Hence,

$$\mathbf{K}_l \Delta\mathbf{d}_l^n = \mathbf{F}_l^{\text{ext},n+1} - \mathbf{f}_l \quad (22)$$

where \mathbf{K}_l is the local consistent tangent stiffness matrix given by

$$\mathbf{K}_l = \mathbf{K}_g + \mathbf{G}_2^T + \mathbf{G}_2 - \mathbf{H}_{22} + (\mathbf{M}_\kappa + \mathbf{G}_1 - \mathbf{H}_{12})^T \mathbf{H}_{11}^{-1} (\mathbf{M}_\kappa + \mathbf{G}_1 - \mathbf{H}_{12}) \quad (23)$$

and \mathbf{f}_l is the local internal force vector

$$\mathbf{f}_l = \mathbf{G}_1^T \mathbf{f}_s^n + \int_L \mathbf{N}_{S_2}^T (\hat{\mathbf{e}}^n - \mathbf{e}^n) dx + (\mathbf{M}_\kappa + \mathbf{G}_1 - \mathbf{H}_{12})^T \mathbf{H}_{11}^{-1} \mathbf{E}_C^n \quad (24)$$

3.5 Nonlinear state determination algorithm

The nonlinear system of equations is iteratively solved using Newton's method using three imbricated loops at different levels (structural level, element level and cross-section level). The local element strain-displacement compatibility equation $\mathbf{E}_C = \mathbf{0}$ is solved iteratively for every global equilibrium iteration. Similarly, the local cross-section constitutive equation $\mathbf{S}_Q = \mathbf{0}$ is solved iteratively at the cross-section level for every element compatibility level iteration. Therefore, residuals at the cross-section equilibrium and element compatibility levels are eliminated through iterations at each of these levels. In this subsection, the superscripts n, i and j denote the iteration indices for the global structural equilibrium, the element compatibility and the cross-section equilibrium levels, respectively. Before launching the computer program (initialization), the local displacement vector for each finite element and the generalized strains \mathbf{e} at each Gauss point along the element length, need to be stored as zero vectors. Once the local displacements are obtained, the state determination procedure, established to obtain the internal force vector and tangent stiffness matrix in the local frame, starts as follows:

1. Evaluate the generalized strains $\hat{\mathbf{e}}$ compatible with the interpolated displacements \mathbf{d}_l

$$\hat{\mathbf{e}}^n = \hat{\mathbf{e}}(\mathbf{d}_l^n)$$

2. Evaluate the nodal force degrees of freedom \mathbf{f}_s . (iterate on $\Delta \mathbf{f}_s^i$)

$$\Delta \mathbf{f}_s^i = \mathbf{H}_{11}^{-1} \mathbf{E}_C^i, \mathbf{f}_s^{i+1} =: \mathbf{f}_s^i + \Delta \mathbf{f}_s^i \text{ where } \mathbf{E}_C^i = \int_L \mathbf{N}_{S_2}^T (\hat{\mathbf{e}}^n - \mathbf{e}^i) dx$$

3. Evaluate the generalized stress resultant internal force vector \mathbf{S}

$$\mathbf{S}^{i+1}(\mathbf{f}_s^{i+1}) = \mathbf{N}_{S_1} \mathbf{f}_s^{i+1}$$

4. Cross-section equilibrium level : Consider for the first iteration at this level that $\mathbf{e}^j =: \mathbf{e}^i$, then, evaluate the generalized strains \mathbf{e} derived from the interpolated stress-resultant force fields

$$\Delta \mathbf{e}^j = \mathbf{q}(\mathbf{S}^{i+1}(\mathbf{f}_s^{i+1}) - \mathbf{S}_\Sigma^j(\mathbf{e}^j)), \mathbf{e}^{j+1} =: \mathbf{e}^j + \Delta \mathbf{e}^j \text{ where } \mathbf{S}_\Sigma^j(\mathbf{e}^j) = \int_A \mathbf{A}^T \boldsymbol{\sigma}(\mathbf{A} \mathbf{e}^j) dA$$

5. Repeat the above step until $\|\mathbf{S}^{i+1} - \mathbf{S}_\Sigma^{j+1}\| \leq \text{tolerance}$, then consider $\mathbf{e}^{i+1} =: \mathbf{e}^{j+1}$ upon convergence.
6. Repeat the above steps from 2 to 5 until $\|\mathbf{E}_C^{i+1}\| \leq \text{tolerance}$, then consider $\mathbf{f}_s^n =: \mathbf{f}_s^{i+1}, \mathbf{e}^n =: \mathbf{e}^{i+1}$ and $\mathbf{E}_C^n =: \mathbf{E}_C^{i+1}$ upon convergence.
7. Calculate local element forces \mathbf{f}_l and tangent stiffness matrix \mathbf{K}_l

4 EXAMPLES

4.1 Cantilever with channel-section

Figure 2 contains the problem description. This example was first introduced by Gruttmann et al. [7]. The beam is modeled using 4 bmw3d elements and the results are compared against 4 and 20 pbw3d displacement-based beam elements. These meshes used 2 Gauss points per element length and 80 integration points within the cross-section. In Figure 2, the load versus the vertical displacement v of point O at the cantilever tip is depicted, where the nonlinear response has been computed up to $v = 200$. The results obtained with 4 bmw3d and 20 pbw3d elements are in very good agreement with those presented by [7] based on shell elements. Furthermore, the results obtained with 4 pbw3d elements do not agree well over a large extend of the computed load deflection curve. It can be observed that, in elasto-plasticity, the number of mixed-based beam elements used to discretize the structure is considerably reduced compared to the number of displacement-based beam elements needed to obtain the load-displacement curve with the same accuracy. This problem demonstrates the capability of the mixed formulation to satisfactorily predict the nonlinear behavior of beams with nonsymmetric cross-sections.

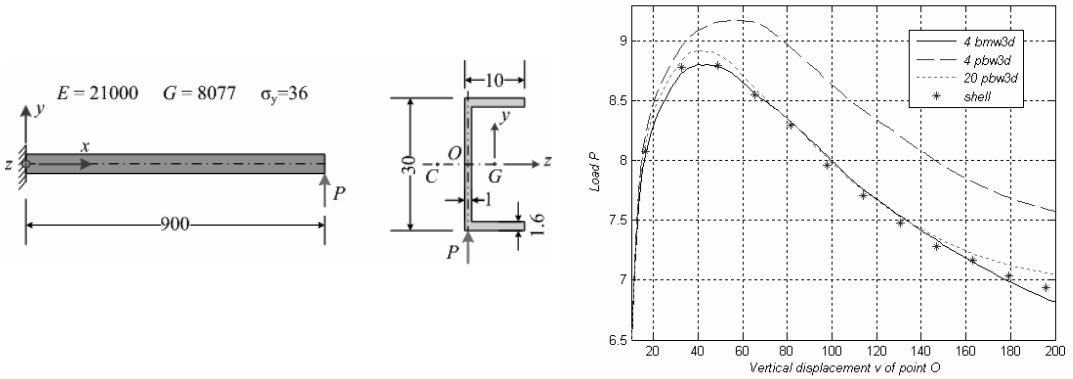


Figure 2: Cantilever with channel-section: data and results.

4.2 Right-angle frame

The right-angle frame, shown in Figure 3 is subjected to a concentrated out-of-plane load P acting at the middle of the span of the horizontal member. In the first model, each member is modeled using 4 *bmw3d* elements with 3 Gauss integration points along the element length. The square cross-section is meshed into a grid of 64 integration points. Four and 20 *pbw3d* elements per member are also used for the second and third models, respectively, with the same element and cross-section discretization. Nonlinear analysis is also performed with *FineLg* [9], using 20 corotational two-noded spatial beam elements. The load versus the out-of-plane displacement of point O curves are depicted in Figure 3 for all models. The comparison between the models shows a very good agreement between the results obtained with the mixed model and those obtained with *FineLg* and with 20 *pbw3d* displacement-based elements per member.

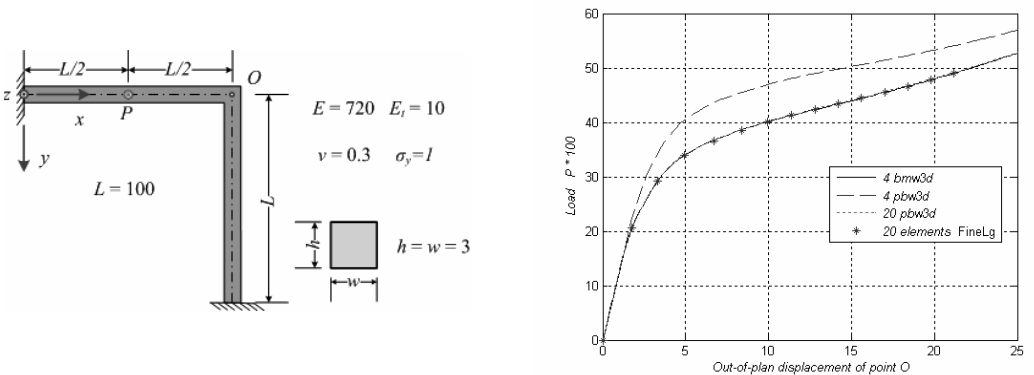


Figure 3: Right-angle frame: data and results.

5 CONCLUSION

This paper proposed an efficient local mixed finite element formulation for the analysis of 3D Bernoulli beams with small strains and large displacements and rotations. The corotational technique proposed in [4] is employed here. The local strains are derived based on a consistent second-order linearization of the fully geometrically nonlinear Bernoulli beam theory. A 3D, geometric-nonlinear, elasto-plastic local beam element based on the incremental form of the two-field Hellinger-Reissner

functional has been presented. This element is targeted particularly for the analysis of thin-walled beams with generic open cross-section where the centroid and shear center of the cross-section are not necessarily coincident. Several numerical examples have demonstrated the superiority of the mixed formulation over displacement-based one: the use of mixed formulation leads to a considerable reduction in the number of elements needed to perform the analysis with the same accuracy.

REFERENCES

- [1] Izzuddin B.A., Smith D.L. "Large-displacement analysis of elasto-plastic thin-walled frames. I: Formulation and implementation". *Journal of Structural Engineering (ASCE)*, **122**(8), 905-914, 1996.
- [2] Alsafadie R., Battini J.-M., Somja H., Hjiatj M. "Local formulation for elastoplastic corotational thin-walled beams based on higher-order curvature terms". *Finite Elements in Analysis and Design*, submitted.
- [3] Alsafadie R., Battini J.-M., Hjiatj M. "Efficient local formulation for elasto-plastic corotational thin-walled beams". *Communications in Numerical Methods in Engineering*, in press.
- [4] Battini J.-M., Pacoste C. "Co-rotational beam elements with warping effects in instability problems". *Computer Methods in Applied Mechanics and Engineering*, **191**(17), 1755-1789, 2002.
- [5] Battini J.-M., Pacoste C. "Plastic instability of beam structures using co-rotational elements". *Computer Methods in Applied Mechanics and Engineering*, **191**(51), 5811-5831, 2002.
- [6] Crisfield M.A., Moita G.F. "A unified corotational framework for solids, shells and beams". *International journal of Solids and Structures*, **33**(20-22), 2969-2992, 1996.
- [7] Gruttmann F., Sauer R., Wagner W. "Theory and numerics of three-dimensional beams with elastoplastic material behavior". *International Journal for Numerical Methods in Engineering*, **48**(12), 1675-1702, 2000.
- [8] Van Erp G.M., Menken C.M., Veldpaus F.E. "The nonlinear flexural-torsional behavior of straight slender elastic beams with arbitrary cross-sections". *Thin-Walled Structures*, **6**(5), 385-404, 1988.
- [9] FineLg User's Manual. V9.0. Greisch Info S.A. - Department ArGEnCo - Liege University (ULg), 2005.